SECED 2023 Conference
Earthquake Engineering & Dynamics for a Sustainable Future
14-15 September 2023, Cambridge, UK

INVESTIGATING LONG AND SHORT-TERM TIME DEPENDENCIES IN EARTHQUAKE RISK MODELLING

Salvatore IACOLETTI[1], Gemma CREMEN[2] & Carmine GALASSO[3]

Abstract: *State-of-practice earthquake risk modelling involves several important simplifications, which neglect (1) interactions between adjacent faults; (2) the long-term elastic-rebound behaviour of faults; (3) the short-term hazard increase associated with aftershocks; and (4) damage accumulation in assets due to the occurrence of multiple earthquakes in a short time window. Several recent earthquake events (e.g., 2010 Canterbury earthquakes, New Zealand; 2019 Ridgecrest earthquakes, USA; 2023 Turkey-Syria earthquakes) have emphasised the need for models to account for the aforementioned short- and long-term time-dependent characteristics of earthquake risk. This work specifically investigates the sensitivity of earthquake risk metrics to these time dependencies for a case study portfolio in Central Italy. The end-to-end approach for time-dependent earthquake risk modelling used in this study incorporates (a) recent advancements in long-term time-dependent fault modelling and aftershock forecast; (b) vulnerability models that account for damage accumulation due to multiple ground motions occurring in a short time; and (c) consideration of time-dependent catastrophe risk insurance features. The sensitivity analysis results provide valuable guidance on the importance and appropriate treatment of time dependencies in regional (i.e., portfolio) earthquake risk models. We found that the long-term fault modelling and whether or not aftershocks are accounted for are the most important features to constrain in a time-dependent seismic risk model. If a large proportion of the assets in the portfolio has a high deductible, then accounting for damage accumulation also becomes important.*

Introduction

Several recent earthquake events (e.g., 2010-12 moment-magnitude – M_W – 7.1-6.2 Christchurch sequence, New Zealand; 2019 M_W 6.4–7.1 Ridgecrest sequence, USA; 2023 Turkey-Syria M_W 7.8–7.5 sequence) have emphasised the need to explicitly account for time dependencies in seismic risk assessments. This is because short-term (i.e., months to years) space-time clustering of earthquakes after large mainshocks can cause significant amplification of damage and loss due to (a) the relatively large ground-motion shaking intensities that aftershocks can produce (e.g., Papadopoulos and Bazzurro, 2020; Iacoletti et al., 2022a); and (b) the increased vulnerability of building stock/infrastructure systems after the main event (e.g., Kam et al., 2011). The occurrence of mainshocks is also governed by long-term (i.e., decades to centuries) time-dependent mechanisms such as (a) elastic rebounding (Reid, 1910), i.e., faults cyclically accumulating elastic strain energy and releasing it when the fault rocks' internal strength/capacity is reached; and (b) stress-based fault-interaction triggering, which causes longterm clustering of large mainshocks (Toda et al., 1998). Yet, the current state of practice in seismic risk assessment involves some significant simplifications that neglect the aforementioned timedependent features of earthquake risk. The implications of these simplifications on risk calculations are typically investigated separately (or at least non-exhaustively), neglecting their combined effects. For instance, Porter et al. (2017) performed a sensitivity study with the longterm time-dependent version of the Uniform California Earthquake Rupture Forecast (UCERF3, Field et al. 2014),

[1] PhD Candidate, Department of Civil, Environmental and Geomatic Engineering, University College London, London, UK, salvatore.iacoletti@ucl.ac.uk
[2] Lecturer, Department of Civil, Environmental and Geomatic Engineering, University College London, London, UK
[3] Full Professor, Department of Civil, Environmental and Geomatic Engineering, University College London, London, UK, and Scuola Universitaria Superiore (IUSS), Pavia, Italy

exploring the effect of elastic rebound behaviour on financial risk (monetary loss) estimates for the state of California. Papadopoulos and Bazzurro (2020) accounted for both aftershocks and damage accumulation (the latter considered in a simplified fashion) when

investigating monetary loss estimates for a region in Central Italy. These studies further underline the importance of time dependency in seismic risk assessment.

This study provides a more comprehensive investigation of the effects of time dependencies in earthquake risk models. An end-to-end simulation-based time-dependent earthquake risk assessment framework for building portfolio is leveraged, integrating:

1. Recent advancements in long-term time-dependent fault modelling, as outlined in Iacoletti et al. (2021). These include the elastic-rebound-motivated methodologies of the latest UCERF3 and explicit consideration of fault-interaction triggering between major known faults;
2. Modelling of short-term hazard increases after large mainshocks. This is carried out with the Epidemic-Type Aftershock Sequence (ETAS) model, calibrated using a recent technique recently proposed by Iacoletti et al. (2022b);
3. State-dependent fragility and vulnerability models calibrated in Iacoletti et al. (2023), capturing the impact of damage accumulation due to multiple ground motions.

The investigation is specifically designed to provide important insights for the catastrophe (CAT) insurance and reinsurance industry. It also considers the hours clause, a time-dependent feature of current insurance policies for earthquake risk. This clause stipulates that the insurer will cover all financial losses accumulated in a defined number of hours after a catastrophic event begins. Accurately modelling the implications of this clause in CAT risk models is challenging, given the lack of standardisation in insurance practices in assigning loss claims to specific hours or events (Mitchell-Wallace, 2017). Because of these challenges, insurers are becoming more interested in understanding the impact of hours clauses on losses. To the best of the authors' knowledge, this study is the first to explore such an issue.

Our study focuses on monetary loss metrics for a sample portfolio in Central Italy. These metrics cover both ground-up loss (the total amount of loss incurred before applying any insurance or reinsurance financial structures) and gross loss (the loss to the insurer after limits and deductibles are applied but before any form of reinsurance is accounted for). We use common loss metrics such as the Average Annual Loss (AAL, also known as pure premium or expected annual loss) and the return-period (RP) loss values (also known as Value-at-Risk).

Methodology

Simulation-based time-dependent earthquake risk assessment framework

Figure 1 outlines the simulation-based time-dependent earthquake risk assessment framework used in this study. The framework follows the general structure of a conventional catastrophe risk model (i.e., hazard, exposure, vulnerability and financial modules; Mitchell-Wallace, 2017). Timedependent components are represented as a series of input options, which are subsequently investigated through sensitivity analyses (Section "Variance-based sensitivity analysis").

The seismic hazard module generates stochastic event sets (i.e., synthetic catalogues of earthquake ruptures) as specified in Iacoletti et al. (2022a), based on simulated seismicity for the region of interest over a number of years. Either a time-independent (TI) or a time-dependent rupture occurrence model can be selected. The time-dependent rupture occurrence model is the Brownian Passage Time (BPT; Matthews et al., 2002) model. The stochastic event sets can also account for fault interaction (fi) or not ($f\bar{i}$). Fault interaction is modelled by introducing a stressbased proxy (i.e., Coulomb stress changes; Mignan et al. 2016) that modifies the rupture occurrence probabilities computed with the rupture occurrence model (Iacoletti et al., 2021). Aftershocks may be generated (as) or not ($a\bar{\bar{s}}$) with the ETAS-based aftershock simulator included. All simulated earthquakes in the stochastic event sets include rupture information required for the ground-motion intensity calculations (e.g., location, magnitude, and nodal planes).

The exposure module contains a portfolio of assets associated with a specific building type (i.e., taxonomy). This information is then used to select appropriate vulnerability models in the vulnerability module. The ground-up expected loss ratio for each asset and each earthquake, $E(LR_{gu,a,e})$ (where the loss ratio is the estimated repair cost divided by the replacement cost), is

calculated from the vulnerability model based on the ground-motion fields generated for the asset's location. Two alternative approaches to vulnerability modelling are used:

- The conventional approach (indicated with $\bar{\bar{\bar{dacc}}}$) used in seismic risk assessments, in which the vulnerability calculations do not account for damage accumulation. This means that the vulnerability module has no memory of the building's existing damage state due to previous events, and the $E(LR_{gu,a,e})$ is evaluated independently for each earthquake with the same vulnerability model (i.e., the assets are considered repaired immediately after each ground motion);
- The approach proposed by Iacoletti et al. (2023) (indicated with $dacc$), which uses statedependent vulnerability and fragility models to capture damage and loss accumulation due to multiple ground motions. State-dependent fragility models define the probability that a damaged structure (after one or a series of ground motions) will reach or exceed a certain ith damage state (ds_i) following a subsequent ground motion of a prescribed intensity (e.g., Aljawhari et al., 2020). State-dependent vulnerability models define the $E(LR_{gu,a,e})$ of an initially damaged building (i.e., which reached a certain ds_j during previous ground motions). Further details on this approach can be found in Iacoletti et al. (2023).

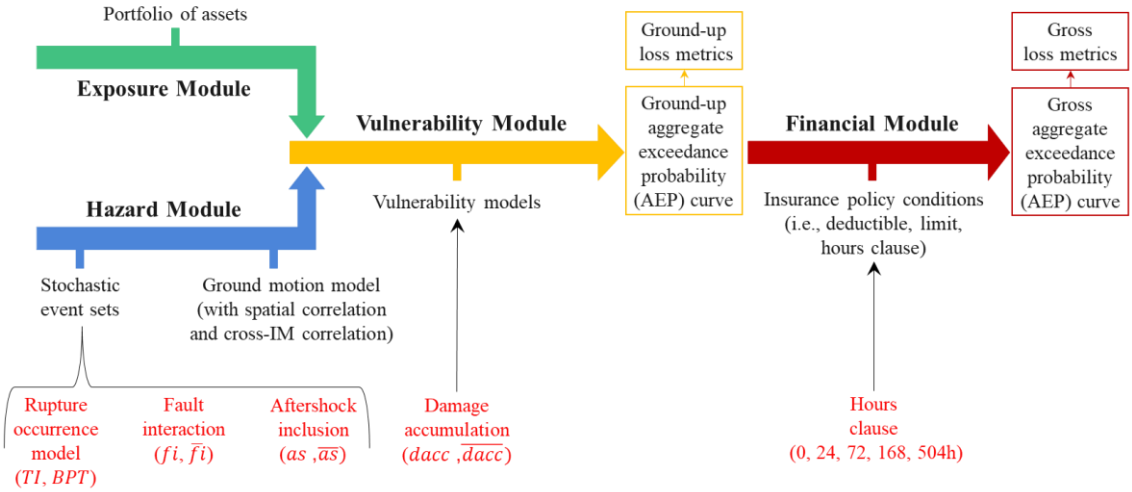

Figure 1. Flowchart of the simulation-based time-dependent earthquake risk assessment framework used in this study. Time-dependent input options are displayed in red font.

The expected asset-level ground-up loss related to each earthquake, $E(L_{gu,a,e})$, is calculated by multiplying the corresponding $E(LR_{gu,a,e})$ by the replacement cost of each asset. The uncertainty around $E(LR_{gu,a,e})$ is neglected for simplicity. This assumption is not expected to affect the conclusions of this study, as we focus on the relative sensitivity of loss metrics rather than absolute loss estimates. The expected portfolio ground-up loss for an earthquake, $E(L_{gu,e})$, is then the sum of the $E(L_{gu,a,e})$ of each asset in the portfolio. The annual portfolio ground-up loss, $E(L_{gu})$, for each simulated year of the stochastic event set is calculated as the sum of the $E(L_{gu,e})$ values. The aggregate exceedance probability (AEP) curve is calculated as outlined in MitchellWallace (2017) and provides the probability of the sum of event losses in a year ($E(L_{gu})$ in the case of ground-up losses) exceeding a certain loss level. Commonly used loss metrics derived from the $E(L_{gu})$ AEP curve (Mitchell-Wallace, 2017) include ground-up AAL (indicated AAL_{gu} and calculated as the integral under the $E(L_{gu})$ AEP curve, Goda et al., 2015), and specific-RP $E(L_{gu})$ (i.e., the $E(L_{gu})$ corresponding to a specific RP in the $E(L_{gu})$ AEP curve).

The hours clause input option to the financial module is implemented for each asset and the nth simulated year of the stochastic event set, according to the following procedure:

1. Identify the events occurring within the nth year;
2. Order the identified events according to their associated $E(LR_{gu,a,e})$ value, from highest to lowest;
3. Iterate over each ordered event (referred to as a payout event):
    a. If the event belonged to the hours clause window of a previous payout event, skip the next two steps and relabel the event as a "cumulative event" (see next step);
    b. Identify other simulated earthquakes (referred to as cumulative events) within the hours clause window, starting from the timestamp of the payout event;

c. Add the $E(LR_{gu,a,e})$ of the cumulative events to that of the payout event, to produce $E(LR_{gu,a,e})^*$.

The expected asset-level gross loss ratio, $E(LR_{gr,a,e})$, is calculated by applying insurance limits and deductibles to each asset's $E(LR_{gu,a,e})^*$. The deductible is the amount of loss a policyholder has to pay before reclaiming from the policy; the insurance limit is the maximum amount a policy will pay out (both are expressed as a percentage of the replacement cost). The expected assetlevel gross loss related to each payout event, $E(L_{gr,a,e})$, is calculated by multiplying the corresponding $E(LR_{gr,a,e})$ by the replacement cost of each asset. The expected portfolio gross loss for each earthquake, $E(L_{gr,e})$, is the sum of the $E(L_{gr,a,e})$ of each asset in the portfolio. Complex reinsurance treaties can also be implemented to share $E(L_{gr,e})$ among different stakeholders. The annual portfolio ground-up loss, $E(L_{gr})$, for each simulated year of the stochastic event set is calculated as the sum of the $E(L_{gr,e})$ values. $E(L_{gr})$ AEP curve and loss metrics (e.g., gross AAL, indicated with AAL_{gr}) are then computed.

Variance-based sensitivity analysis

We conduct variance-based sensitivity analysis to investigate the effects of introducing time dependencies in earthquake risk models. For a given model of the form $Y = g(X)$, variance-based methods quantify the sensitivity of Y to X in terms of a reduction in the variance of Y (e.g., Saltelli et al., 2010). In this study, Y is the loss metric of interest (such as AAL_{gu} or AAL_{gr}), the function $g(\cdot)$ represents the methodology used in this study to calculate losses (i.e., Section "Simulationbased time-dependent earthquake risk assessment framework"), and X represents the input options of Figure 1. The first-order (main) sensitivity coefficient S_i is used to estimate the contribution of the ith input to the output variance (i.e., it measures the effect of varying the ith input alone, averaged over variations in other input parameters). Consistent with the methodology in Saltelli et al. (2010), four matrices are generated: (1) $\boldsymbol{A}$, built with S samples of each of the input options; (2) $\boldsymbol{B}$ with an additional S samples generated in the same way as $\boldsymbol{A}$; (3) $\boldsymbol{C_i}$, built by substituting the ith column of matrix $\boldsymbol{A}$ for the ith column of matrix $\boldsymbol{B}$; and (4) $\boldsymbol{D_i}$, built by substituting the ith column of matrix $\boldsymbol{B}$ for the ith column of matrix $\boldsymbol{A}$. Matrices $\boldsymbol{A}$ and $\boldsymbol{B}$ are sampled independently, while matrices $\boldsymbol{C_i}$ and $\boldsymbol{D_i}$ are built from $\boldsymbol{A}$ and $\boldsymbol{B}$ (respectively) to investigate the variance of Y due to the ith input change. The ith subscript of $\boldsymbol{C_i}$, and $\boldsymbol{D_i}$ relates to the ith changed column (i.e., input) with respect to $\boldsymbol{A}$ and $\boldsymbol{B}$, respectively. Each row of each matrix is used to sample K-years stochastic events sets and compute AEP curves and loss metrics (see Section "Simulation-based time-dependent earthquake risk assessment framework"). Y_A, Y_B, Y_{Ci}, and Y_{Di} are vectors of a given loss metric corresponding to $\boldsymbol{A}$, $\boldsymbol{B}$, $\boldsymbol{C_i}$, and

$\boldsymbol{D_i}$, respectively. The first-order (main) sensitivity coefficient, S_i, is estimated as specified in Saltelli et al. (2010).

Case study

We used the bounding box of longitudes [13°, 13.9°] and latitudes [41.9°, 42.8°] in Central Italy to carry out the sensitivity analysis (Figure 2). The sensitivity results are presented for the entire portfolio described in Section "Exposure module", as well as for the cities of L'Aquila, Teramo and Avezzano specifically (i.e., only considering assets in these cities), which collectively represent around 40% of the portfolio's total replacement value.

Seismic hazard module

The stochastic event sets used in the case study have been developed by Iacoletti et al. (2022a) for Central Italy in the bounding box of longitudes [12.6°, 14.2°] and latitudes [41.6°, 43.2°]. Iacoletti et al. (2022a) built the hazard module by combining (a) a fault-based seismicity module; (b) a distributed seismicity module; and (c) an ETAS-based aftershock simulator. The fault-based seismicity model comprises 43 fault segments, shown in Figure 2. Fault data needed to calibrate the fault-based seismicity module (i.e., slip rates, paleoseismic records, date of the last event) is taken from Scotti et al. (2021). Consistent with Field et al. (2015), the BPT model is considered with different levels of recurrence uncertainty: high (BPT_{high}), medium (BPT_{mid}), or low (BPT_{low}). The Homogenized Instrumental Seismic Catalog (HORUS, Lolli et al., 2020) is used to calibrate the parameters of the ETAS-based aftershock simulator according to Iacoletti et al. (2022b).

The ground-motion fields for each simulated earthquake are generated by sampling the groundmotion model (GMM) proposed by Cauzzi et al. (2015) at the location of the assets in the portfolio, also using site-specific information on the shear-wave velocity in the upper 30 m (V_{S30}).

The intraevent residuals are simulated, accounting for both spatial and cross-correlation, using the procedure proposed by Markhvida et al. (2018).

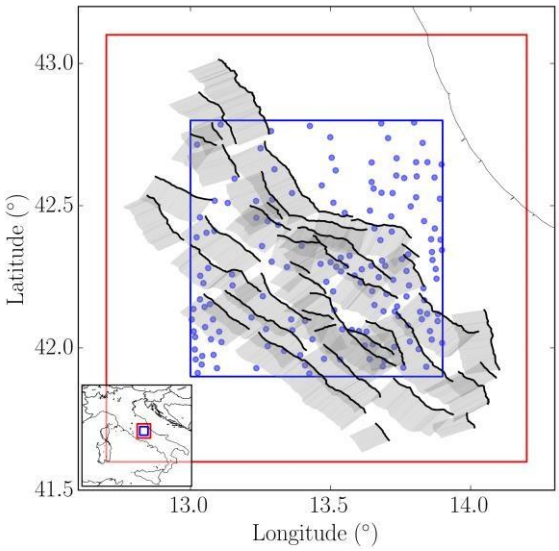

Figure 2. Case-study portfolio (subset of that of Crowley et al. 2021 within the blue polygon). The red polygon is the study area used in Iacoletti et al. (2022a) to generate the stochastic event sets. The 43 considered fault segments are shown in black (fault trace) and grey (geometry at depth).

Exposure module

The case-study portfolio (shown in Figure 2) is a subset of that in the European Seismic Risk Model 2020 (ESRM20, Crowley et al., 2021). The number of buildings and associated total replacement costs (structural, non-structural and contents) of the ESRM20 portfolio for Italy were aggregated at administrative level 3 (i.e., roughly equivalent to a township or a municipality) and represented by a density-weighted centroid, which is calculated from the built-up area density map (Crowley et al., 2021). Each centroid is associated with assets of different building types, which identify the (a) material of the lateral load resisting system (LLRS); (b) LLRS type; (c) seismic code or ductility level, and (d) building height (following the approach proposed by Martins and Silva, 2020). This building stock contains around 136,000 buildings, 32 different building types, and a total replacement cost of €27.4 Billion.

Vulnerability models

We use the suite of single-ground-motion (i.e., mainshock-only) and state-dependent fragility and vulnerability models developed by Iacoletti et al. (2023) for the building types used in this study (https://github.com/SalvIac/sequence_frag_vuln). The IM associated with each state-dependent and single-ground-motion (i.e., mainshock-only) fragility and vulnerability model is the average spectral acceleration at a range of periods of interest (which vary for each building type), calculated from the capacity curve associated with each taxonomy (Martins and Silva, 2020; Iacoletti et al., 2023). ds_i range from ds_0 to ds_3, representing no (ds_0), slight (ds_1), moderate (ds_2), or extensive (ds_3) damage (Martins and Silva, 2020).

Ground-up losses

Figure 3 provides the uniformly-weighted logic tree with the time-dependent input options investigated. S=2,000 and K=10,000-yr are used in this study as they produce numerically stable S_i values for the investigated loss metrics. Figure 4 displays the $E(L_{gu})$ AEP curves for some logic tree branches (i.e., $\bar{\bar{as}}$-$\bar{\bar{dacc}}$-TI-$\bar{fi}$, $\bar{\bar{as}}$-$\bar{\bar{dacc}}$-BPT_{mid}-$\bar{fi}$ and as-$dacc$-BPT_{mid}-fi), as well as the range of variability of these curves across all 32 branches shown in Figure 3. Figure 4 also provides the ratio (for each specific annual probability of exceedance) of the as-$dacc$-BPT_{mid}-fi and $\bar{\bar{as}}$-$\bar{\bar{dacc}}$-BPT_{mid}-$\bar{fi}$ curves with respect to $\bar{\bar{as}}$-$\bar{\bar{dacc}}$-TI-$\bar{fi}$. The time-dependent rupture occurrence model leads to lower values of $E(L_{gu})$ in general; the AAL_{gu} for $\bar{\bar{as}}$-$\bar{\bar{dacc}}$-BPT_{mid}-$\bar{fi}$ is approximately 9% less than that for $\bar{\bar{as}}$-$\bar{\bar{dacc}}$-TI-$\bar{fi}$. This is because the time-dependent rupture occurrence probability of the considered fault system in Central Italy is lower than that calculated with a time-independent model (Iacoletti et al., 2022a). Aftershock inclusion, fault interaction, and the inclusion of state-dependent vulnerability calculations (denoted by as-$dacc$-BPT_{mid}-fi) lead to an increase in AAL_{gu} of around 22% relative to $\bar{\bar{as}}$-$\bar{\bar{dacc}}$-BPT_{mid}-$\bar{fi}$, and an increase of approximately

25% in the 200-year-RP $E(L_{gu})$. These increases are mostly due to the inclusion of the aftershocks, which considerably amplify hazard (and potential losses) following relatively large-magnitude mainshocks.

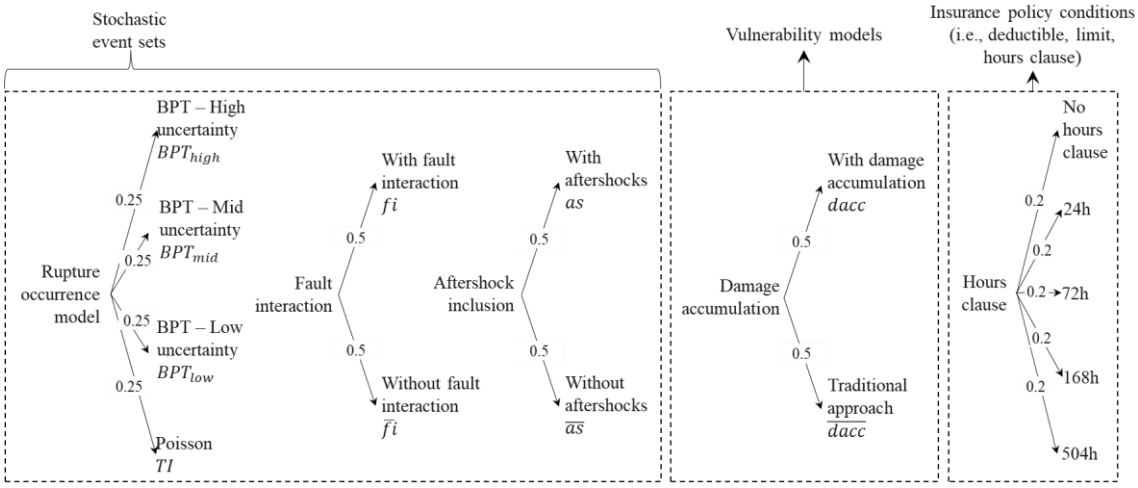

Figure 3. Logic tree for the sensitivity analysis.

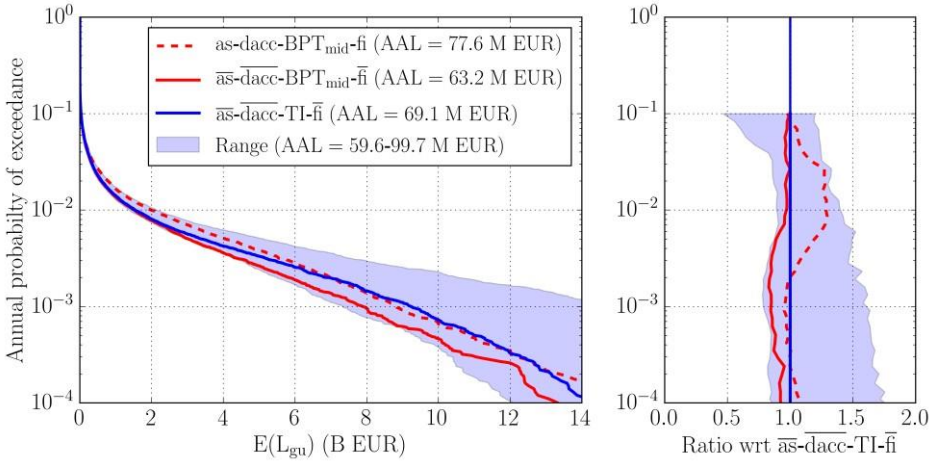

Figure 4. Left panel: $E(L_{gu})$ AEP curves for $\overline{\overline{as}}$-$dacc$-TI-$f\bar{i}$, $\overline{\overline{as}}$-$\overline{\overline{dacc}}$-$BPT_{mid}$-$f\bar{i}$ and as-$dacc$-BPT_{mid}-fi, and the range of variability across all 32 branches of the considered logic tree. Right panel: ratio of the as-$dacc$-BPT_{mid}-fi and $\bar{\bar{a}}\bar{s}$-$dacc$-BPT_{mid}-$f\bar{i}$ AEP curves with respect to the AEP curve for $\overline{\overline{as}}$-$\overline{\overline{dacc}}$-$TI$-$f\bar{i}$, and the range of variability of these ratios across all 32 branches of the considered logic tree.

Figures 5 provides the S_i values associated with the AAL_{gu} and 2500-year-RP $E(L_{gu})$ (denoted as $S_{i,AAL}$ and $S_{i,RP2500}$, respectively) for the cities of L'Aquila, Teramo and Avezzano, and the entire portfolio. S_i values associated with fault interaction modelling are close to negligible in all cases. This is consistent with the findings of Iacoletti et al. (2022a) for the same region. It is explained by the fact that typical ruptures generated by the 43 considered fault segments (Figure 2) cannot produce stress changes large enough to affect the occurrence probabilities of other ruptures (Iacoletti et al., 2021). However, this result is highly dependent on the specific details of the case study, including fault geometry and earthquake magnitudes. The $S_{i,AAL}$ values associated with vulnerability modelling are generally small. The corresponding $S_{i,RP2500}$ values are larger, implying that the consideration (or not) of damage accumulation is more important in the tail of the $E(L_{gu})$ AEP curve (corresponding to high RP $E(L_{gu})$ values).

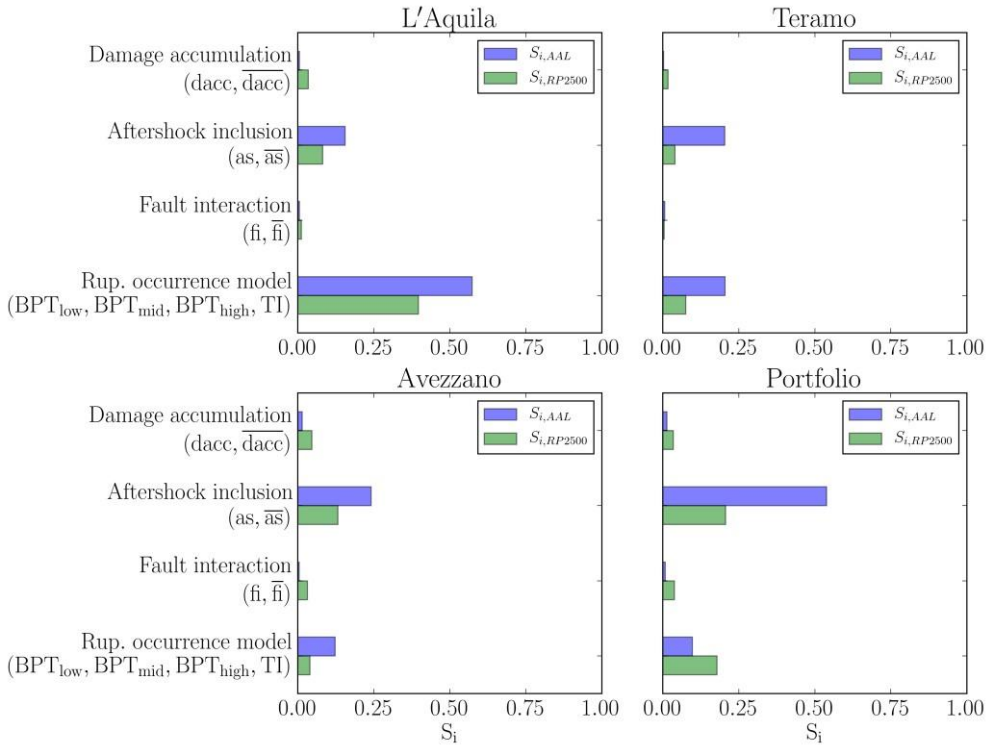

Figure 5. $S_{i,AAL}$ and $S_{i,RP2500}$ for the cities of L'Aquila, Teramo and Avezzano, and the entire case-study portfolio.

The AAL_{gu} and 2500-year-RP $E(L_{gu})$ are most sensitive to variations in the rupture occurrence models (i.e., time-dependent versus time-independent models) and the inclusion (or not) of aftershocks. At L'Aquila, the highest $S_{i,AAL}$ and $S_{i,RP2500}$ values are associated with rupture occurrence modelling. This is because time-dependent seismic hazard at this location is expected to be lower than the time-independent case due to the rupture of the Paganica fault in 2009 (e.g., Pace et al., 2016; Iacoletti et al., 2022a). At Teramo, the highest $S_{i,AAL}$ value is associated with aftershock modelling (although the $S_{i,AAL}$ value associated with rupture occurrence modelling is only slightly smaller) and the highest $S_{i,RP2500}$ is associated with rupture occurrence modelling. For both Avezzano and the overall portfolio, the highest $S_{i,AAL}$ and $S_{i,RP2500}$ values are associated with aftershock modelling (although the overall portfolio $S_{i,RP2500}$ value for rupture occurrence modelling is similar to that for aftershock modelling). The 2500-year-RP $E(L_{gu})$ of the overall portfolio is more sensitive than the AAL_{gu} to variations in the rupture occurrence models. This reflects the fact that the choice of rupture occurrence model most affects rare, longer term hazard estimates (Iacoletti et al., 2022a). The inclusion or not of aftershocks affects short-term hazard estimates, which helps to explain why the corresponding $S_{i,AAL}$ value is generally higher than that of the corresponding $S_{i,RP2500}$.

Gross losses

The sensitivity of gross loss metrics is investigated for five hours-clause windows (see Figure 3): 0 (equivalent to no hours clause), 24, 72, 168, and 504 hours, using three levels of deductible (set respectively as 0.1%, 1% and 10% of the replacement cost of each asset). The insurance limit is set to 100% of the replacement cost of each asset. Reinsurance measures are not included in this study for simplicity. Figure 6 provides the variance-based sensitivity results associated with the AAL_{gr} of the entire portfolio, for the different deductibles investigated. Consistent with the sensitivity ground-up loss metrics, the consideration of fault interaction has a limited effect on the variance of the AAL_{gr}. The rupture occurrence model $S_{i,AAL}$ values remain reasonably constant across different deductibles and indicate that AAL_{gr} is as sensitive as AAL_{gu} to this modelling feature. The $S_{i,AAL}$ value associated with the hours clause is generally low and increases with the deductible. The $S_{i,AAL}$ values associated with aftershock modelling are relatively high, except for a 10% deductible. This is because higher deductibles are less frequently exceeded for aftershocks. The $S_{i,AAL}$ value for state-dependent vulnerability is highest for a 10% deductible because this deductible level is more frequently exceeded when damage accumulation is accounted for.

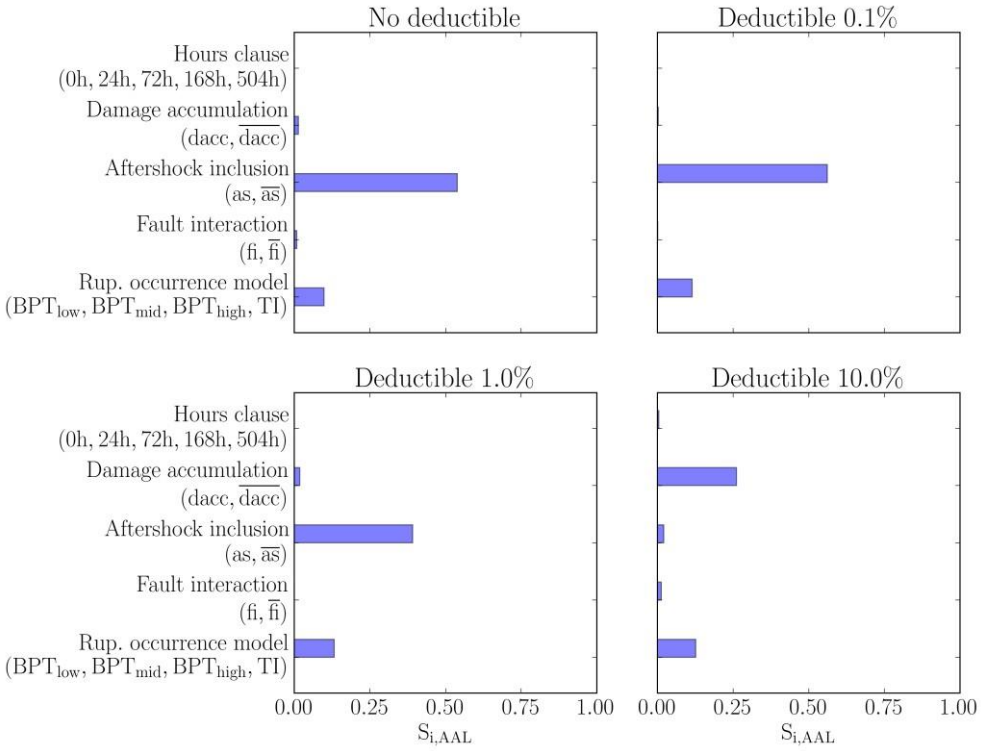

Figure 6. $S_{i,AAL}$ of the AAL_{gr} for the entire case-study portfolio and different deductibles.

Conclusions

This study explored the sensitivity of monetary loss metrics to various time dependencies often neglected in conventional earthquake risk models. A simulation-based time-dependent earthquake risk assessment framework was used to carry out the sensitivity analysis, accounting for (a) long-term time-dependent rupture occurrence models, which describe the elastic-rebound behaviour of faults; (b) fault-interaction triggering mechanisms between major known faults; (c) short-term hazard increases due to aftershocks occurring after large mainshocks; and (d) damage accumulation due to multiple ground motions occurring in a short time period. The monetary loss metrics used in this study are the Average Annual Loss (ground up, AAL_{gu}, and gross, AAL_{gr}) and specific- RP portfolio loss values (ground-up, $E(L_{gu})$, and gross, $E(L_{gr})$). The investigation was designed to provide important insights for the catastrophe insurance and reinsurance industry, so specific insurance features (e.g., hours clauses) are also considered in the $E(L_{gr})$ calculations. A sample portfolio in Central Italy, including the cities of L'Aquila, Teramo and Avezzano, was used as a case study for the investigation.

The sensitivity analysis revealed that the ground-up versions of both examined loss metrics are most sensitive to the choice of long-term rupture occurrence model and whether or not aftershocks are accounted for. Thus, these two modelling features are the most important to constrain when developing a time-dependent seismic risk model (at least for the case study investigated). The AAL_{gu} metric is generally more sensitive to the modelling of aftershocks than the 2500-year-RP $E(L_{gu})$. This is because aftershocks increase short-term hazard estimates and corresponding losses at low RP. Time-dependent rupture occurrence models can also significantly affect AAL_{gu} close to a fault that recently ruptured (e.g., at L'Aquila). Sensitivity of specific-RP $E(L_{gu})$ to aftershock modelling decreases with increasing RP, whereas sensitivity to rupture occurrence modelling exhibits the reverse trend. This means that the choice of rupture occurrence model is more important than the aftershock consideration for large-RP $E(L_{gu})$ (including the 2500-year-RP $E(L_{gu})$ metric specifically examined). The sensitivity of the loss metrics to the modelling of vulnerability is low compared to the modelling of aftershocks. Still, it increases with increasing RP, for which even larger mainshock events cause considerable initial damage and enable subsequent aftershocks to produce large losses. The sensitivity of the ground-up loss metrics to fault interaction was found to be low, which means that this modelling feature is the least important to constrain in a time-dependent seismic risk model.

Sensitivity results were generally similar for the gross loss metrics examined. The sensitivity of these metrics to the length of the hours clause is low. As the level of deductible considered increases, the sensitivity of AAL_{gr} to the modelling of aftershocks and damage accumulation,

decreases and increases, respectively. This means that for AAL_{gr} the long-term rupture occurrence model and whether or not aftershocks are accounted for are the most important features to constrain in a time-dependent seismic risk model. However, if a large proportion of the assets in the portfolio has a high deductible (around 10% for the considered case study), then accounting for damage accumulation also becomes important.

The findings of this study are limited in applicability to the case studies and ranges of input parameters considered. For instance, the calculation of $E(L_{gr})$ depends on the details of the implementation of the hours clause. The process insurers use for assigning loss claims to specific hours or events is not standardised across the industry; hence, the implementation procedure could be refined to better match the practices of specific insurers. The methodology used in this study could be extended by additionally considering reinsurance treaties (and associated reinstatement clauses). Nevertheless, the sensitivity results obtained provide some valuable guidance on the treatment and importance of time dependencies in advanced large-scale (i.e., portfolio) earthquake risk models.

Acknowledgements

Salvatore Iacoletti was supported by the UK Engineering and Physical Sciences Research Council (EPSRC), Industrial Cooperative Awards in Science & Technology (CASE) grant (Project reference: 2261161) for University College London and Willis Towers Watson (WTW), through the Willis Research Network (WRN). Input to and feedback on the study by Dr Crescenzo Petrone, Dr Umberto Tomassetti, and Dr Myrto Papaspiliou from Gallagher Re is greatly appreciated.

References

Aljawhari K, Gentile R, Freddi F and Galasso C (2020), Effects of Ground-Motion Sequences on Fragility and Vulnerability of Case-Study Reinforced Concrete Frames. *Bulletin of Earthquake Engineering*

Cauzzi C, Faccioli E, Vanini M, and Bianchini A (2015), Updated predictive equations for broadband (0.01–10s) horizontal response spectra and peak ground motions, based on a global dataset of digital acceleration records. *Bulletin of Earthquake Engineering*, 13 (6), 1587–1612.

Crowley H, Dabbeek, Despotaki, Rodrigues, Martins, Silva, Romao, Pereira, Weatherill, and Danciu, 2021. *European Seismic Risk Model (ESRM20)*. Technical report

Field EH, Arrowsmith RJ, Biasi GP, Bird P, Dawson TE, Felzer KR, Jackson DD, Johnson KM, Jordan TH, Madden C, Michael AJ, Milner KR, Page MT, Parsons T, Powers PM, Shaw BE, Thatcher WR, Weldon RJ, and Zeng Y (2014). Uniform California Earthquake Rupture Forecast, Version 3 (UCERF3)–The Time-Independent Model. *Bulletin of the Seismological Society of America* 104, 1122–1180.

Field EH, Biasi GP, Bird P, Dawson TE, Felzer KR, Jackson DD, Johnson KM, Jordan TH, Madden C, Michael AJ, Milner KR, Page MT, Parsons T, Powers PM, Shaw BE, Thatcher, WR, Weldon RJ and Zeng Y (2015), Long-Term Time-Dependent Probabilities for the Third Uniform California Earthquake Rupture Forecast (UCERF3). *Bulletin of the Seismological Society of America* 105, 511–543.

Goda K, Wenzel F and Daniell JE (2015), Insurance and Reinsurance Models for Earthquake. In *Encyclopedia of Earthquake Engineering*, pp. 1184–1206. Springer, Berlin, Heidelberg. ISBN 978-3-642-35344-4.

Iacoletti S, Cremen G and Galasso C (2021), Advancements in Multi-Rupture Time-Dependent Seismic Hazard Modeling, Including Fault Interaction. *Earth-Science Reviews* 220, 103650.

Iacoletti S, Cremen G and Galasso C (2022a), Integrating Long and Short-Term Time Dependencies in Simulation-Based Seismic Hazard Assessments. *Earth and Space Science* 9, e2022EA002253.

Iacoletti S, Cremen G and Galasso C (2022b), Validation of the Epidemic-Type Aftershock Sequence (ETAS) Models for Simulation-Based Seismic Hazard Assessments. *Seismological Research Letters.*

Iacoletti S, Cremen G and Galasso C (2023). Modeling Damage Accumulation during GroundMotion Sequences for Portfolio Seismic Loss Assessments. *Soil Dynamics and Earthquake Engineering* 168, 107821.

Lolli B, Randazzo D, Vannucci G, and Gasperini P (2020), The Homogenized Instrumental Seismic Catalog (HORUS) of Italy from 1960 to Present. *Seismological Research Letters* 91, 3208–3222.

Kam WY, Pampanin S, Elwood K (2011), Seismic performance of reinforced concrete buildings in the 22 February Christchurch (Lyttelton) earthquake. *Bulletin of the New Zealand Society for Earthquake Engineering* 44, 239–278.

Markhvida M, Ceferino L and Baker JW (2018), Modeling Spatially Correlated Spectral Accelerations at Multiple Periods Using Principal Component Analysis and Geostatistics. *Earthquake Engineering & Structural Dynamics* 47, 1107–1123.

Martins L and Silva V (2020), Development of a Fragility and Vulnerability Model for Global Seismic Risk Analyses. *Bulletin of Earthquake Engineering*

Matthews MV, Ellsworth WL and Reasenberg PA (2002). A Brownian Model for Recurrent Earthquakes. *Bulletin of the Seismological Society of America* 92, 2233–2250.

Mignan A, Danciu L and Giardini D (2016). Considering Large Earthquake Clustering in Seismic Risk Analysis. *Natural Hazards*

Mitchell-Wallace, K. (ed.), (2017), *Natural Catastrophe Risk Management and Modelling: A Practitioner's Guide*. John Wiley and Sons, Inc, Hoboken, NJ. ISBN 978-1-118-90604-0.492

Pace B, Visini F and Peruzza L (2016). FiSH : MATLAB Tools to Turn Fault Data into Seismic Hazard Models. *Seismological Research Letters* 87, 374–386.

Papadopoulos AN and Bazzurro P (2020), Exploring Probabilistic Seismic Risk Assessment Accounting for Seismicity Clustering and Damage Accumulation: Part II. Risk Analysis. Earthquake Spectra 37, 386–408

Porter K, Field E and Milner K (2017), Trimming a Hazard Logic Tree with a New Model-OrderReduction Technique. *Earthquake Spectra* 33, 857–874.

Reid H (1910), The Mechanism of the Earthquake, The California Earthquake of April 18, 1906. *Report of the Research Senatorial Commission*, Carnegie Institution, Washington, DC 2, 16–18.

Saltelli A, Annoni P, Azzini I, Campolongo F, Ratto M, and Tarantola S (2010), Variance Based Sensitivity Analysis of Model Output. Design and Estimator for the Total Sensitivity Index. *Computer Physics Communications* 181, 259–270.

Scotti O, Visini F, Faure Walker J, Peruzza L, Pace B, Benedetti L, Boncio P, and Roberts G (2021), Which Fault Threatens Me Most? Bridging the Gap Between Geologic DataProviders and Seismic Risk Practitioners. *Frontiers in Earth Science* 8, 750.

Toda S, Stein RS, Reasenberg PA, Dieterich JH, and Yoshida A (1998), Stress Transferred by the 1995 Mw = 6.9 Kobe, Japan, Shock: Effect on Aftershocks and Future Earthquake Probabilities. Journal of Geophysical Research: Solid Earth 103, 24543–24565.